High-performance x-ray spectroscopic devices for plasma microsources investigations

Physica Scripta. Vol. 50, 333–338, 1994

High-Performance X-ray Spectroscopic Devices for Plasma Microsources Investigations

A. Ya. Faenov,* S. A. Pikuz,** A. I. Erko,*** B. A. Bryunetkin,* V. M. Dyakin,* G. V. Ivanenkov,** A. R. Mingaleev,** T. A. Pikuz,* V. M. Romanova** and T. A. Shelkovenko**

* NPO VNIIFTRI, Mendeleevo, Moscow region, Russia
** P. N. Lebedev Physical Institute, Moscow, Russia
*** Institute for Microelectronic Technology, Chernogolovka, Moscow region, Russia

Received January 27, 1994; accepted in revised form March 17, 1994

Abstract

X-ray spectroscopy with high spectral (up to $\Delta\lambda/\lambda = 10^{-4}$) and spatial resolution (up to 1 μm) is discussed. Devices based on crystals, diffraction and Bragg–Fresnel elements and their applications in Z- and X-pinches and laser plasma experiments are described.

1. Introduction

X-ray spectroscopic techniques enable measuring the most important plasma parameters [1]. The 1–100 Å range wavelength is of primary interest in the development of spectroscopic methods of plasma diagnostics. In particular, plasma parameters vary within very wide limits during compression and expansion of the plasma filament in studies on fast Z-pinches [2] and laser produced plasma. High spatial and spectral resolution and high efficiency are required to obtain adequate information on plasma parameters. Here, we discuss the methods of high-resolution and imaging spectroscopies by using crystals and artificial X-ray optical elements. Experimental results were obtained by means of these devices on BIN facility [3], a laser produced plasma installation and other plasma installations.

2. Devices based on crystals

2.1. *Spectrographs with slits*

Crystals, having in accordance with the Bragg equation spatial resolution in the direction of dispersion, may be used to obtain two-dimensional plasma images in "light" of a separate spectral line. Spatial resolution in this case depends on spectral line width and may be better than 100 μm. This is most fruitful in experiments with large plasma objects in powerful machines like Angara-5 [4] and expanding laser plasma. Figures 1 and 2 show experimental results obtained by spectrographs with convex mica crystals and a slit or diaphragm in front of a crystal for spatial resolution in the transverse direction. Similar devices with CsAP crystals were widely used in X-pinch experiments [5] on BIN machine and in laser plasma experiments [6]. For line and its profile measurements with high spectral resolution, we used Johann-type spectrographs [7]. The accuracy of wavelength measurements was 10^{-3} Å or better.

2.2. *Spherically curved crystals*

High spectral and spatial resolution may be obtained by using spectrographs with spherically curved crystals [1]. In

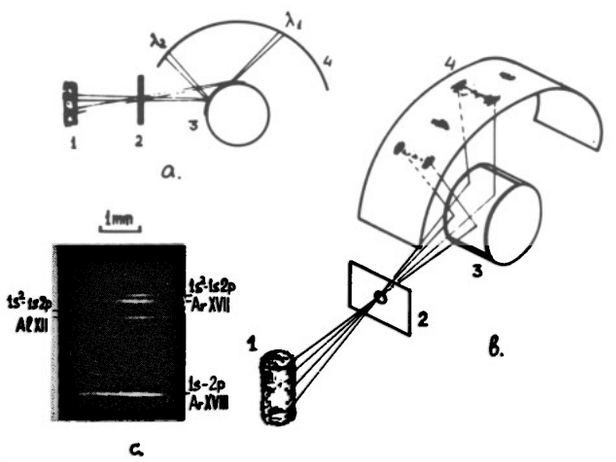

Fig. 1. Convex mica crystal spectrograph with radial spatial resolution in Angara-5 experiment: (a) scheme of spatial resolution forming in dispersion direction, (b) spectrograph scheme (1 – pinch, 2 – pin-hole, 3 – mica crystal, 4 – film), (c) spectrogram of Al/Ar-plasma.

our experiments with laser plasma, we used a quartz crystal (orientation $10\bar{1}0$, $2d = 8.512$ Å) with a 500 mm curvature radius. The laser power density was $\approx 10^{14}$ W/cm^2. The spectral fragment around 8.4 Å wavelengths corresponded to the Lyman doublet of a MgXII ion (Fig. 3). The full width at half maximum (FWHM) of these lines was $\approx 4 \times 10^{-4}$ Å, which corresponds to a spectral resolution $\Delta\lambda/\lambda \approx 0.5 \times 10^{-4}$. This is close to the maximum value determined by the FWHM of a quartz crystal reflection curve.

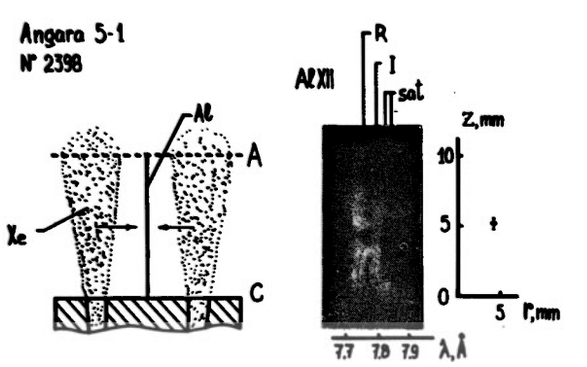

Fig. 2. AlXII spectrum obtained by convex mica crystal spectrograph with axial spatial resolution in Angara-5 experiment. Scheme of experiment (A – anode, C – cathode) and value of spatial resolution are shown.

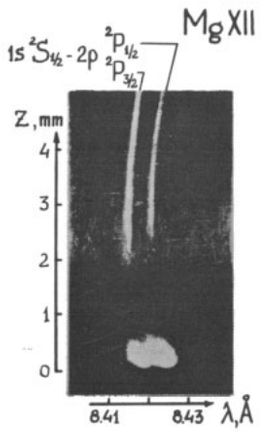

Fig. 3. Emission spectra of laser Mg plasma registered by Johann-type spectrograph with spherically curved quartz crystal [6].

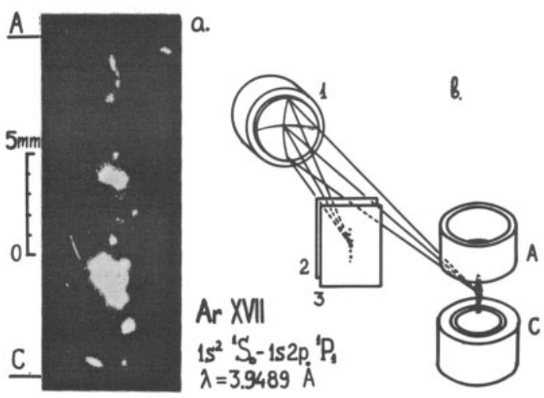

Fig. 4. X-ray microscope in gas-puff experiment [8]: (a) plasma image in He-like Ar ion resonant line; (b) microscope scheme (A – anode, C – cathode; 1 – mount with spherical mica crystal, 2 – filter, 3 – film).

Such instruments have not found wide application, mainly because it has not yet been possible to prepare crystals with a bending radius of less than 300 mm. This limits the detection range and efficiency of the instrument and increases its size. In our study we have constructed spherical analyzers based on mica crystals with bending radius $R = 100$ mm and dimensions 10×30 mm, and with $R = 250$ mm and dimensions 15×50 mm. The high reflectivity of mica in different orders (1–5, 7, 8, 11, 12), combined with its large field of view, makes it possible to cover the large spectral interval from 1.5 to 19 Å. These crystals may be used in an X-microscope scheme [9] (Fig. 4). Another application [10] of this crystal was to create intensive monochromatic collimated beams of soft X-rays in the 4–10 Å spectral range (Figs 5, 6). A comparison of created beam parameters with the parameters of the shortest wavelength X-laser (45-Å Ta-laser [11]) is shown in Table I. Some characteristics (divergency, wavelength, supply energy efficiency) of the obtained beam surpass those of a Ta-laser and some (monochromatization, pulse energy) are a little worse.

2.3. *FSSR spectrograph*

By using spherically curved crystals, one can construct an extremely efficient spectrograph with high spectral and spatial resolution – Focusing spectrograph with Spherical dispersive element and Spatial Resolution (FSSR spectrograph). This scheme was proposed by S. Pikuz and A. Faenov for laser plasma [1] and appears to be very fruitful in other plasma experiments.

Figure 7 shows the setup for using the spherical crystal in the focusing spectrograph mode with spatial resolution. In

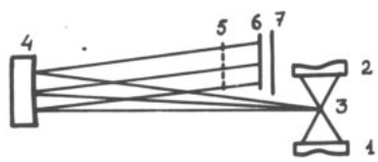

Fig. 5. The scheme of formation of monochromatic collimated beams of soft X-ray radiation with the help of spherical crystal mirrors: 1 – X-pinch anode, 2 – cathode, 3 – plasma hot point, 4 – spherical crystal mirror, 5 – test wire meshes, 6 – filter and X-ray film, 7 – screen that protects from a direct X-ray emission.

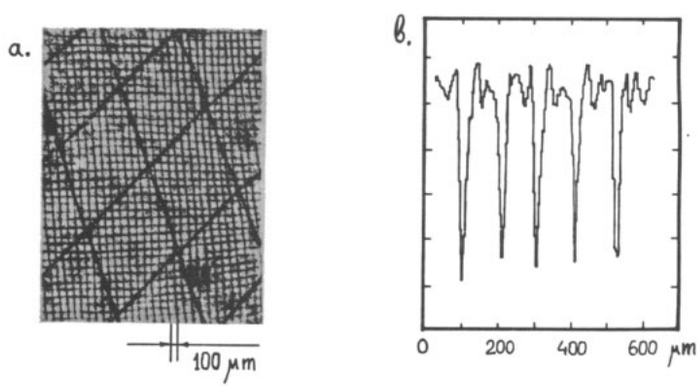

Fig. 6. Photo in X-ray emission of two wire meshes, placed at 2 cm from X-ray film (a) and densitogram of part of smaller wire mesh (b) (X-pinch, Cu-wires, diameter 30 μm).

Table I

Target	X-pinch Cu	X-pinch Pd	Ta-laser Ta
Reflection order of mica crystal	2	5	—
Wavelength, Å	9.8987–9.9389	3.9607–3.9768	45
Monochromatization, $\Delta\lambda/\lambda$	$4 \cdot 10^{-3}$	$4 \cdot 10^{-3}$	10^{-4}
Beam size, mm × mm	10 × 45	10 × 45	0.075 × 0.050
Energy, mJ	3.2×10^{-3}	2×10^{-3}	10^{-2}
The number of photons in pulse	1.6×10^{10}	4×10^{9}	2.3×10^{11}
Duration, nsec	5–10	2–5	0.2
Divergency	$(5 \times 5) \times 10^{-4}$	$(5 \times 5) \times 10^{-4}$	$(1 \times 2) \times 10^{-2}$
Efficiency from supply energy	1.6×10^{-10}	10^{-10}	$(1–2) \cdot 10^{-12}$

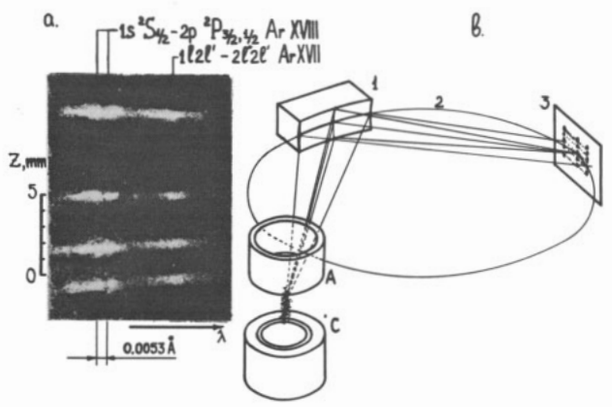

Fig. 7. FSSR spectrograph in gas-puff experiment [8]: (a) spectrum of Ar close to H-like ion resonant line; (b) schematic diagram of space resolved spectrum imaging (A – anode, C – cathode; 1 – mount with spherically bent crystal, 2 – Rowland circle, 3 – film).

this case the spectrum is formed on the Rowland circle in the sagittal plane and the spatial resolution is ensured by focusing in the meridional direction. The magnification in this case is given by $K = b/a = \cos 2\varphi = 2m^2(\lambda/2d)^2 - 1$, where φ is the angle of incidence of radiation on the crystal, $a = R\cos\varphi/\cos 2\varphi$ and $b = R\cos\varphi$ are the distances from source to crystal and from crystal to photographic film, respectively, and d is the interplanar crystal spacing.

In Figs 8–10 spectra obtained by FSSR spectrographs are presented. Spectra of Ti plasma in exploded wires experiments were registered in the 7-th order of mica crystal reflection (Fig. 8). Spectra of He-like TiXXI and satellite spectra of TiXVIII–XX were obtained by using crystals with curvature radius $R = 100$ mm, and $K_{\alpha_{1,2}}$ using $R = 250$ mm. Fine structures of Al- and Cu-wire X-pinches were investigated by using $R = 100$ mm crystals (Figs 9 and 10). In the first case, high resolution of FSSR spectrographs enabled us to measure shapes of lines [Fig. 9(b), (c)] corresponding to transitions from upper levels of H- and He-like Al. In the second case, the high reflectivity of mica crystals in different orders simultaneously (Fig. 10) permitted to register spectra of Ne-like Cu (2-nd order), K_α lines (12-th order) and bremsstrahlung "hot spots" radiation (3-d-7-th orders). In this case, a two-film "sandwich" was used as radiation receiver. The front film (KODAK RAR 2497) registered soft

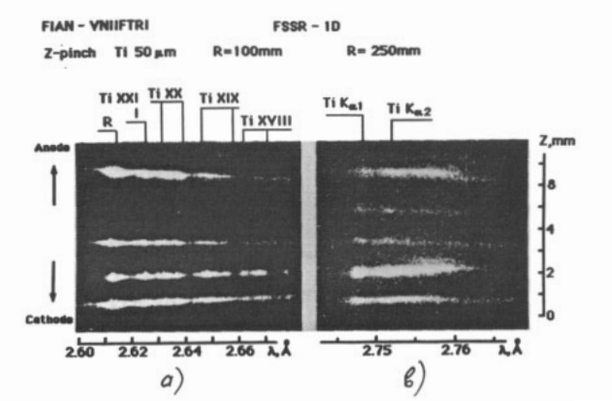

Fig. 8. Spectrograms obtained for various "hot spots" of Z-pinch Ti-wires plasma: (a) spectra near resonance line of He_α obtained by FSSR-1D mica spherical $R = 100$ mm crystal (7-th order of reflection, satellite lines belonging to different isoelectronic sequences are marked), (b) spectra near K_α-line obtained by mica spherical $R = 250$ mm crystal (7-th order of reflection).

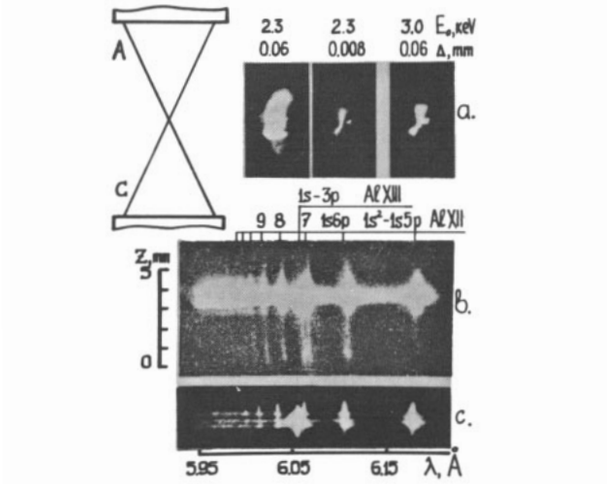

Fig. 9. (a) Schematic illustration of the X-pinch (A – anode, C – cathode) and pinhole photographs of the X-pinch obtained with pinhole of diameter 60 μm covered by filters with various cut-off energies E_0.

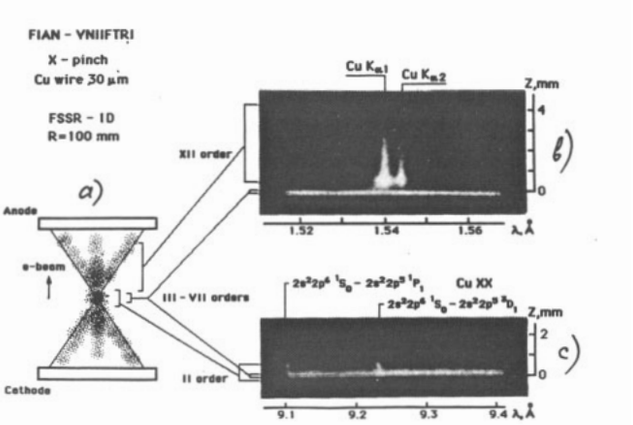

Fig. 10. (a) Schematic illustration of the X-pinch experiment with e-beam generation, (b) spectra near K_α-line of Cu at 12-th order of reflection of mica spherical $R = 100$ mm crystal (the second film; one can clearly see that K_α generation started at some distance from the dense hot spot of X-pinch cross-section) and (c) spectrogram of Ne-liked Cu-ions received simultaneously at the 2-nd order of reflection (first film).

radiation, while the back one (KODAK DEF) hard components with $\lambda < 3$ Å. The highest spatial resolution (18 μm) was experimentally achieved in Pd X-pinch experiments (Fig. 11).

The variant of this scheme (FSSR-2D) with out-off Rowland circle film position enabled to obtain 2-dimensional images of plasma sources (Fig. 12). In this case,

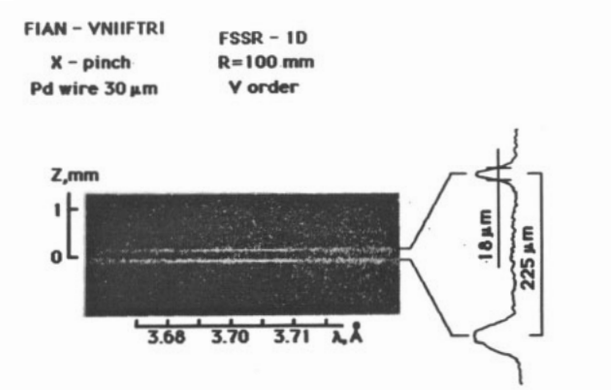

Fig. 11. Image of Pd-wires X-pinch in the 5-th order of reflection of mica spherical $R = 100$ mm crystal.

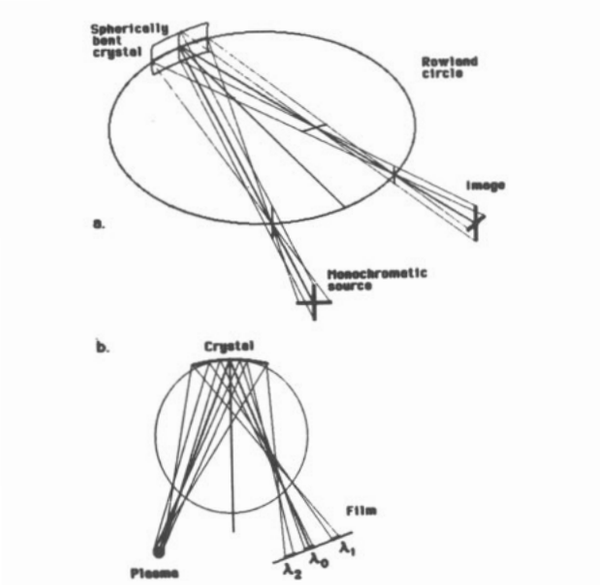

Fig. 12. The schemes of (a) 2D image formation by use of spherically bent crystal and (b) image formation in the direction of dispersion.

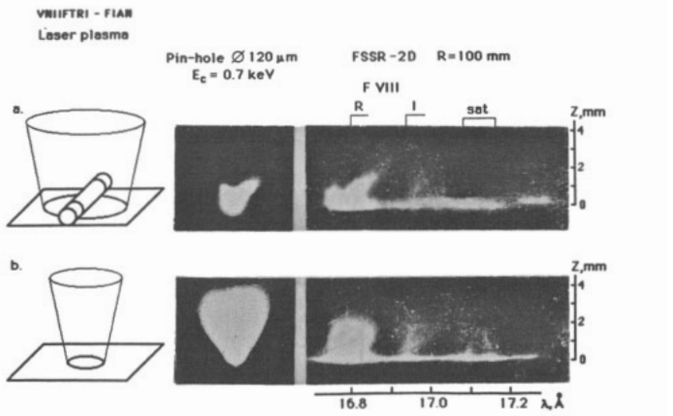

Fig. 14. The structure of radiation of flat CF_2-target (b) and target covered by Fe-wire (diameter 200 μm) (a). One can clearly see the correlation of images obtained by pinhole and FSSR-2D spectrometer with mica spherical R = 100 mm crystal.

the Johann scheme crystal works as a "pin-hole" for separate spectral line radiation in the sagittal plane. Of course, the scheme possesses some specific aberrations (Fig. 13), but it can give fruitful plasma structure information in experiments (Fig. 14). In general, image magnifications are in the transverse direction; for $a = b = R/\cos\varphi$ we have a one-to-one image in both directions. Precisely this situation was realized in Fig. 14.

3. Artificial X-ray optical elements

3.1. *Transmission diffraction grating*

By use of such dispersive elements, one can investigate pinch radiation in a very wide spectral range (5–100 Å) with high spatial, but very rough spectral, resolution. In our study we used a spectrograph with transmission grating [12], which consists of a system of unsupported strips with a 1 μm period, located inside a 25 μm diameter aperture or 0.1 mm × 1 mm slit. Since the membrane in which the grating had been formed was comparatively large (diameter ≈1.5 mm), we placed an auxiliary screen of 50-μm-thick tantalum foil of 40-μm diameter or a 0.15 mm × 1.2 mm diaphragm in front of the grating to prevent direct exposure to hard X-rays (Fig. 15).

2.2. *Bragg–Fresnel multilayer lens (BFML)*

Recent achievements in the X-ray optics domain significantly expand the experimental opportunities in spectral diagnostics of high-temperature plasma sources. The development of artificial X-ray optical elements with volume Fresnel zones [13], BFML, allows not only to overcome the choice restrictions of natural and synthetic crystals that can be used in X-ray devices. BFML also enable to considerably improve some characteristics of such devices, for example, relative aperture and spatial resolution.

BFML with straight structures that provide linear focusing were used in our experiments. These lenses were made by using electron beam lithography, optical lithography, and ion beam etching. The fabricated lens had an aperture of 1 mm × 5.6 mm and a minimum last zone width of 3.5 μm. The BFML were prepared by ion etching a 141 layer of 32 Å period W/Si multi-layer mirror coated by magnetron. This lens had a 7 cm focal distance at a wavelength of 1.54 Å.

The scheme of the experiment and some results are shown in Figs 16 and 17. In this case, the lens was oriented on wavelength 4.5 Å in the third order of reflection. On its

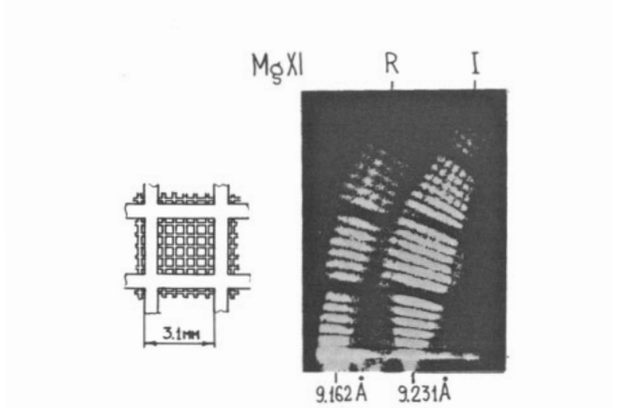

Fig. 13. Image of two overlapping 100 μm and 500 μm wire grids illuminated by laser-produced plasmas (FSSR-2D) spectrograph with mica spherical R = 100 mm crystal).

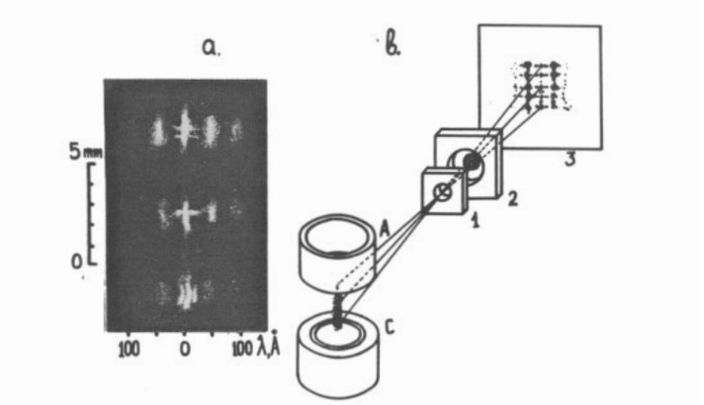

Fig. 15. Transmission grating spectrograph in gas-puff experiment: (a) one shot plasma spectrum; (b) schematic diagram of spectrograph (A – anode, C – cathode; 1 – tantalum diaphragm, 2 – mount with grating, 3 – film).

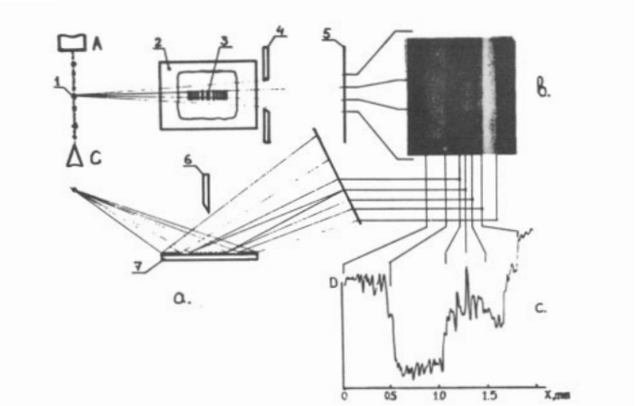

Fig. 16. The scheme of lens operation in emission of $\lambda = 4.5$ Å (a) (1 – plasma hot point of exploded wire, 2 – Bragg structure, 3 – Fresnel lens structure, 4, 6 – screens, 5 – film, 7 – Si substrate; A – anode, C – cathode of high-current diode), plasma image in the 1-st and 3-d diffraction orders (b) and (c) plasma image densitogram.

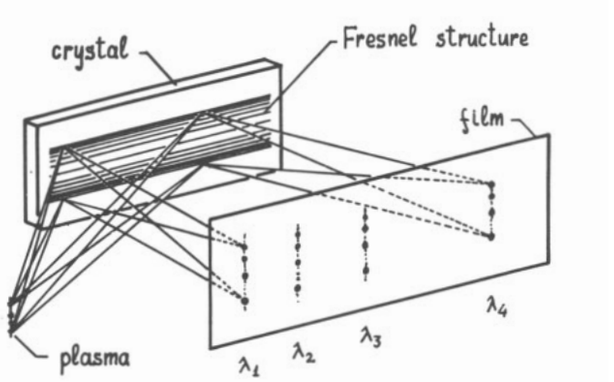

Fig. 18. The scheme of using the linear Bragg–Fresnel lens for obtaining plasma spectra with spatial resolution: 1 – mica crystal, 2 – linear Bragg–Fresnel lens, 3 – film, 4 – pinch.

sides, the lens had a non-etched multilayer formed during fabrication. That is why on the film, there are, in addition to the lens-formed image, wide strips formed by emission reflected from this structure. The plasma image consists of two elements: the narrow 10 μm wide line and a background formed in the first order of diffraction. In Fig. 17, plasma images obtained by BFL in 1.5 Å radiation and by pin-holes with various cut-off energies are presented. In this case, the sizes of plasma hot-spot images did not exceed 20–30 μm.

3.3. *Zonal plate structure on crystal*

The traditional methods with the slit parallel to the dispersion direction do not have a large transmission and can be used if the slit width (and, accordingly, spatial resolution) is more than ≈20–30 μm. By using a Bragg–Fresnel lens, we sought to obtain high-temperature plasma spectra with high spatial resolution over a wide spectral interval.

For this purpose, we calculated and fabricated a linear Bragg–Fresnel lens on a crystal surface. Calculated parameters of this lens were: focal distance $f_0 = 7$ cm at wavelength $\lambda_0 = 7.75$ Å, last zone width 0.5 μm and total aperture ≈1 cm × 108.5 μm. A mica crystal with a $2d = 19.944$ Å lattice period as a substrate was used. A Bragg–Fresnel lens was formed by electron beam lithography and wet etching in a metal layer deposited on the crystal surface. The thickness of the layer was designed to provide π phase shift in the reflected X-ray beam coming through the layer.

The scheme of the experiment with the Bragg–Fresnel lens is shown in Fig. 18. The first Bragg–Fresnel lens was used for obtaining a Z-pinch plasma image in radiation close to the resonant lines of Ne-like ion PdXXXVII. In Fig. 19, you can see the plasma spectrum obtained on the convex crystal spectrograph and the image obtained by using the Bragg–Fresnel lens. In this case, the Bragg–Fresnel lens was arranged so that the image on wavelength $\lambda_0 \sim 4$ Å had a magnification $\gamma_0 = 1.2$.

4. Conclusion

By using the described devices, one can investigate plasma parameters with high spatial and spectral resolution over a wide spectral range. In Table II, a comparison of parameters devices are presented.

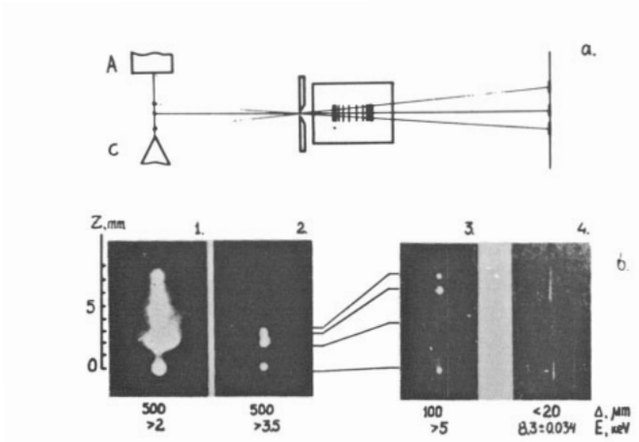

Fig. 17. The scheme of lens operation in emission of $\lambda = 1.5$ Å (a) and the experimental results (b): 1–3 – pin-hole camera images, 4 – lens obtained images (E – filter cut-off energy in pin-hole camera, D – real spatial resolution of pin-hole camera).

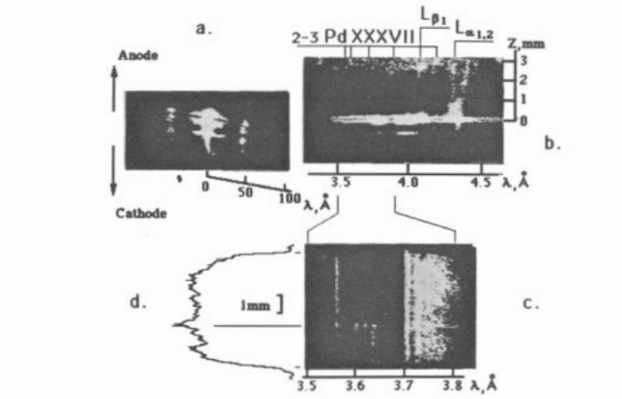

Fig. 19. Experimental results for exploded Pd-wires X-pinch geometry: (a) spectrum obtained by using pinhole transmission grating spectrograph, (b) plasma spectrum obtained by using convex CsAP crystal spectrograph (L – characteristic lines of wire material), (c) plasma spectrum in 3.5–3.8 Å range, (d) densitograms of these spectra in direction of spatial resolution better than 50 μm.

Table II

	1	2	3	4	5
Spectrographs with slits:					
flat crystal	1–20	0.1–0.2	10^{-3}	100	20
convex crystal	1–20	1	10^{-3}	100	20
Johann scheme	1–20	0.05–0.2	10^{-4}	—	20
FSSR spectrograph	1–20	0.05–0.2	10^{-4}	—	10–15
FSSR-2D spectrograph	1–20	0.05–0.2	10^{-3}	100	10–15
X-ray microscope	1–20	0.01	—	5—10	5–10
Devices with artificial elements:					
transmission grating	5–100	1	10^{-2}	—	25
Bragg–Fresnel lens	1–15	0.01	10^{-2}	0.5–1	20
zonal plate structure on crystal	3–20	0.1–0.2	10^{-3}	100	0.5–1

1. Spectral range, Å; 2. Relative spectral range $(\lambda_{max} - \lambda_{min})/2(\lambda_{max} + \lambda_{min})$; 3. Spectral resolution $\Delta\lambda/\lambda$; 4. Spatial resolution in direction of dispersion, μm; 5. Spatial resolution in transverse to dispersion direction, μm

Acknowledgement

This work was supported by Russing Fundamental Science Foundation grant 93-02-15410.

References

1. Boiko, V. A., Vinogradov, A. V., Pikuz, S. A., Skobelev, I. Yu. and Faenov, A. Ya., J. Sov. Laser Res. **6**, 85 (1985).
2. Zakharov, S. M., Ivanenkov, G. V., Kolomenskii, A. A., Pikuz, S. A. and Samokhin, A. I., Sov. J. Plasma Phys. **9**, 271 (1983).
3. Ivanenkov, G. V., Mingaleev, A. R., Pikuz, S. A., Romanova, V. M., Shelkovenko, T. A. and Ermatov, Sh. A., Preprint No 50, (P. N. Lebedev Physical Institute, Moscow 1992).
4. Smirnov, V. P., *et al.*, Proceedings of 3-d Int. Conf. on Dense Z-Pinches (London 1993) F1.
5. Bryunetkin, B. A., *et al.*, Sov. J. Quant. Electron. **23**, 201 (1993).
6. Bryunetkin, B. A., Pikuz, S. A., Skobelev, I. Yu and Faenov, A. Ya., "Laser and Particle Beams", **10**, 849 (1992).
7. Mingaleev, A. R., *et al.*, Kvant. Electron. **20**, 461 (1993) (in Russian) (Sov. J. Quant. Electron. 23, 397 1993).
8. Bartnik, A., Ivanenkov, G. V., Karpinski, L., Pikuz, S. A. and Shelkovenko, T. A., Preprint No 58 Moscow: P. N. Lebedev Physical Institute, 1992; Kvant. Electron. **20**, 1121 (1993) (in Russian) (Sov. J. Quant. Electron. **23**, 1993).
9. Belyaev, L. M., *et al.*, Sov. J. Quant. Electron. **6**, 1121 (1976).
10. Faenov, A. Ya., *et al.*, Sov. J. Quant. Electron. **23**, 394 (1993).
11. MacGowan, B. J., *et al.*, Phys. Rev. Lett. **65**, 420 (1990).
12. Bryunetkin, B. A., Ivanenkov, G. V., Pikuz, S. A., Faenov, A. Ya. and Shelkovenko, T. A., Sov. Tech. Phys. Lett. **17**, 689 (1991).
13. Erko, A. I., J. X-ray Sci. Technol. **2**, 297 (1990).